Glozman et al., http://www.jcb.org/cgi/content/full/jcb.200808124/DC1

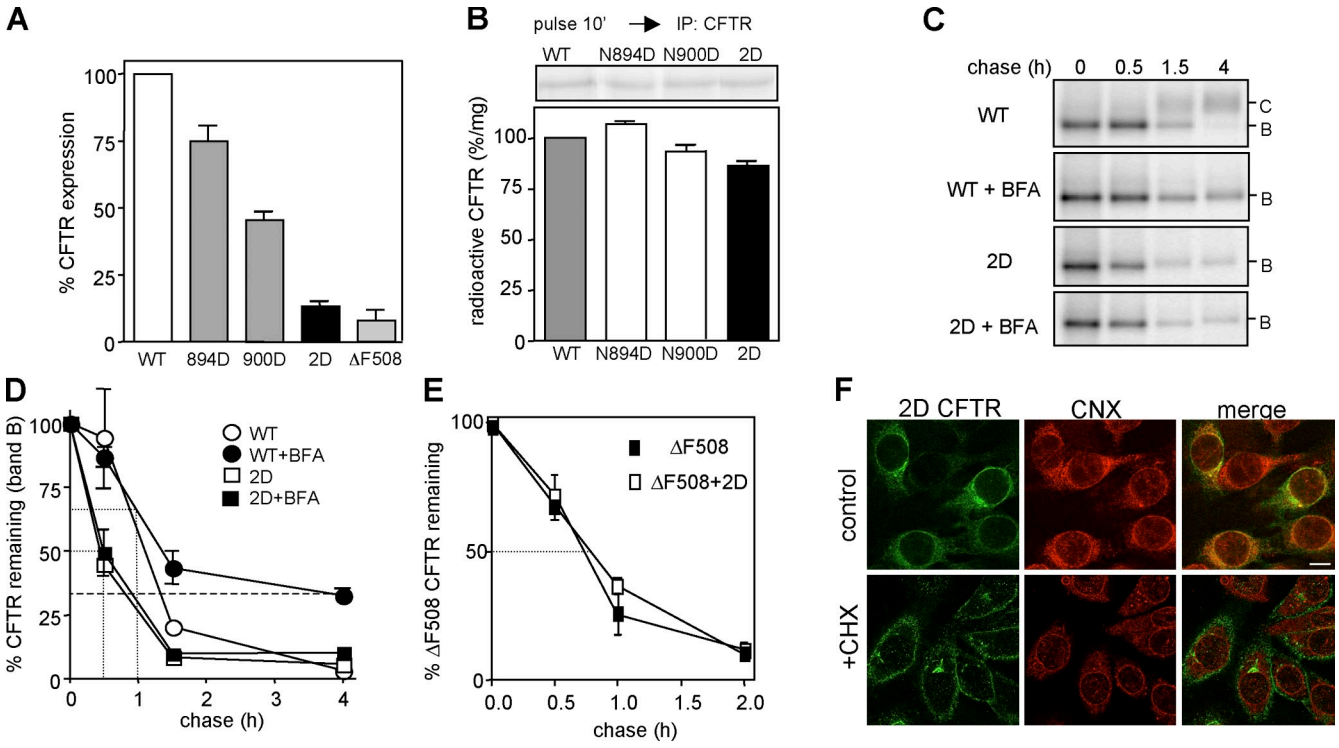

Figure S1. **The effect of N-glycans on CFTR biogenesis.** (A) Densitometric analysis of the steady-state expression level of the glycosylation mutant CFTR. The relative abundance of the complex-glycosylated wt, 894D-, and 900D-CFTR and the nonglycosylated 2D-CFTR was expressed as the percentage of the complex-glycosylated wt CFTR. (B) Translational rates of CFTR variants in BHK cells were measured by the incorporation of [^{35}S]-methionine/cysteine into CFTR during a 10-min pulse. Radioactivity incorporated into CFTR was normalized for cellular protein and expressed as a percent of the wt CFTR. (C and D) The turnover of the wt and 2D-CFTR immature forms was measured by pulse-chase experiment after a 15-min pulse in the presence or absence of 5 µg/ml BFA (mean ± SEM, n = 3). BFA was present during the pulse and chase. Dotted lines indicate the $t_{1/2}$ determination. The dashed line represents the amount of folded core-glycosylated CFTR in the ER. B and C indicate core-glycosylated and complex-glycosylated CFTR, respectively. (E) The turnover rates of the ΔF508- and ΔF508–2D-CFTR were determined in BHK by metabolic pulse technique (n = 3). (F) Monitoring the 2D-CFTR disappearance from the ER. Indirect immunostaining of 2D-CFTR and CNX was visualized by laser confocal microscopy in BHK cells incubated in the presence or absence of 150 µg/ml CHX for 3 h. The gain of the photomultiplier was increased by 10% in the CHX chased sample. IP, immunoprecipitation. Error bars indicate SEM. Bar, 10 µm.

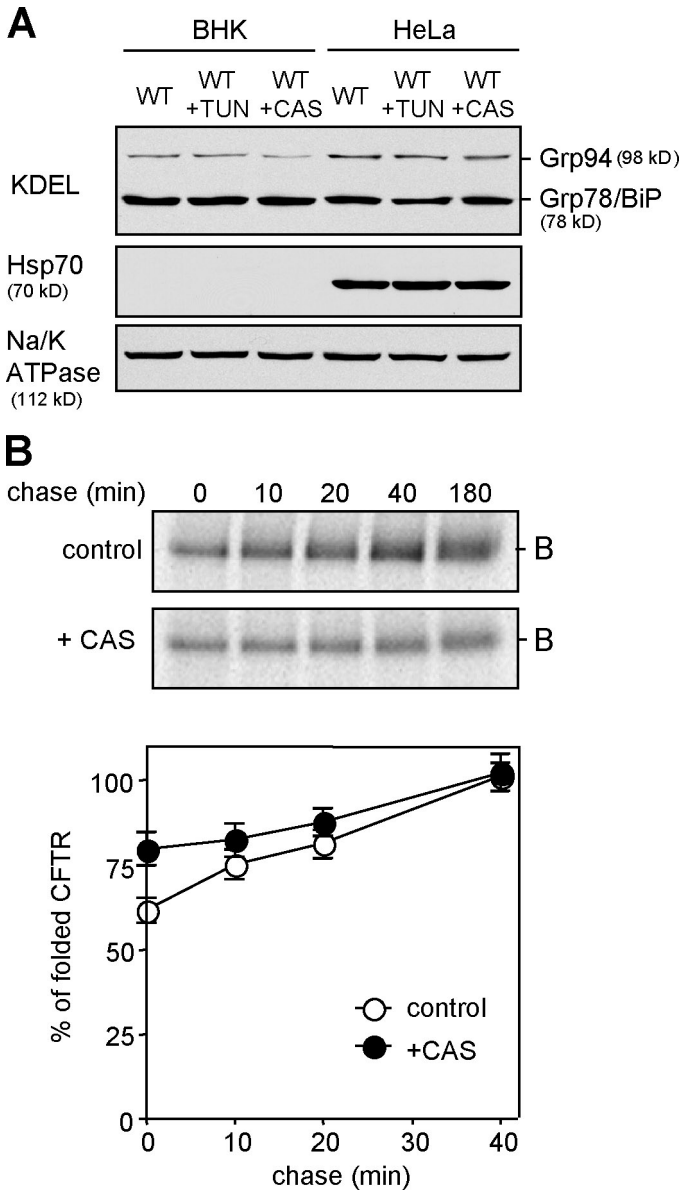

Figure S2. **Effect of CAS and TUN on ER stress and CFTR folding kinetics.** (A) Short treatment of TUN and CAS does not induce ER stress. BHK and HeLa cells expressing wt CFTR-3HA were treated with TUN or CAS as in Fig. 2 C. Grp78/BiP, Grp94, and Hsp70 expression was determined by Western blotting. Na/K-ATPase was used as a loading control. (B) Folding kinetics of CFTR in BHK cells was measured by pulse-chase experiments after 8-min pulse labeling of CFTR and terminating its folding at the indicate chase time by ATP depletion. This was followed by a total 3-h chase in ATP depletion medium to eliminate the incompletely folded CFTR conformers as described previously (Du, K., M. Sharma, and G.L. Lukacs. 2005. *Nat. Struct. Mol. Biol.* 12:17–25.). 1 mM CAS was added during the pretreatment (45 min), methionine depletion (45 min), and pulse labeling. 5 μg/ml BFA was present during the pulse and chase. The increasing amount of radioactivity associated with CFTR reflects the folding process of CFTR completed posttranslationally. The amount of folded CFTR was expressed as the percentage of mature channel after 3-h chase in the absence of ATP depletion. Mean ± SEM, $n = 4$. B indicates core-glycosylated CFTR.

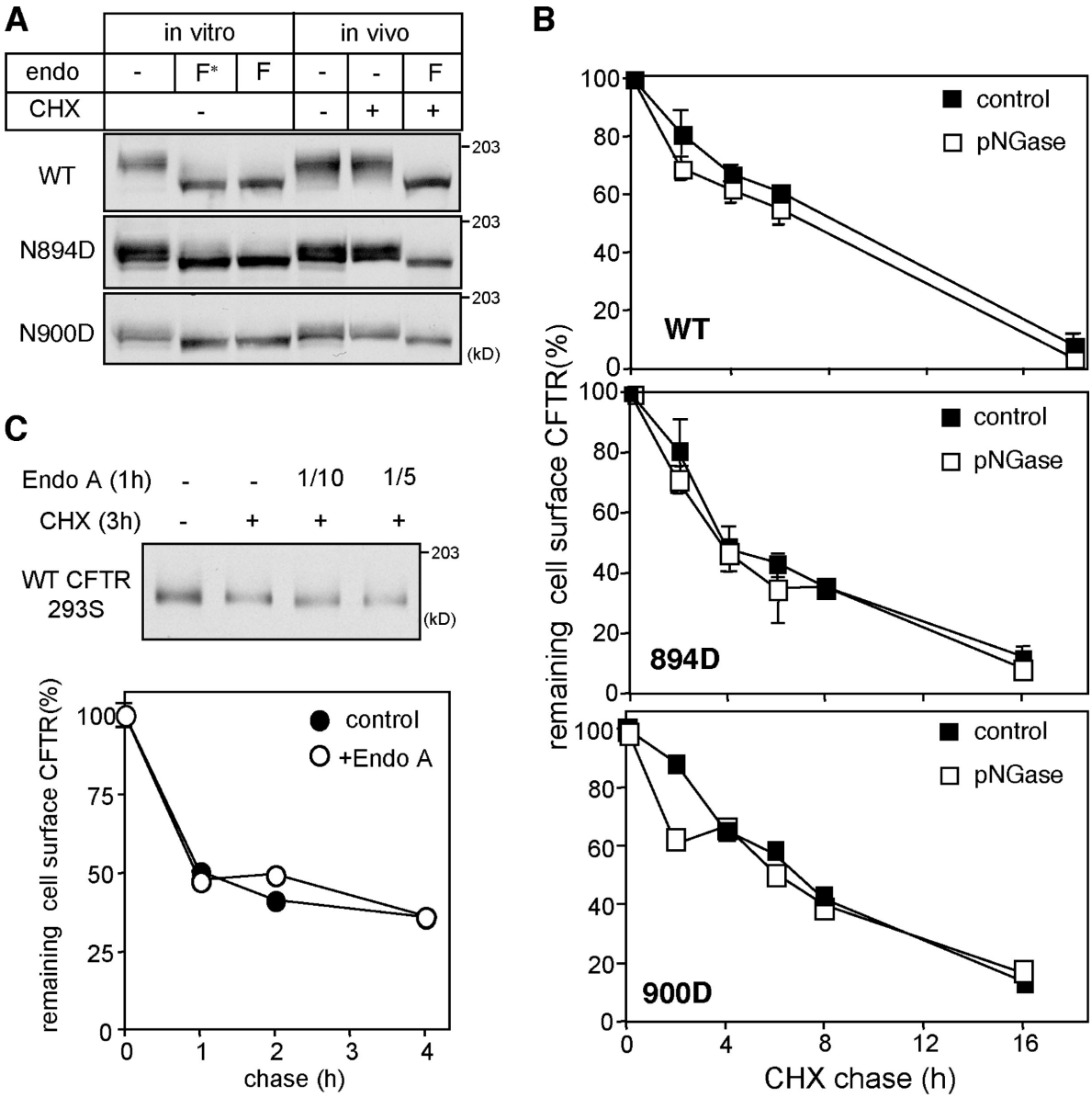

Figure S3. **The effect of N-glycans cleavage on CFTR stability at the cell surface.** (A) Comparison of the in vivo and in vitro glycosidase treatment efficiency. CFTR variants were deglycosylated in vitro (in cell lysate) by 31 μg/ml PNGase (F*; 500 U; New England Biolabs, Inc.) or by 0.5–0.8 mg/ml recombinant PNGase (F; isolated as described in Materials and methods) for 3 h at 33°C. In vivo deglycosylation was accomplished by incubating BHK cells for 3 h at 37°C with 1:50 (vol/vol) 0.5–0.8 mg/ml recombinant PNGase F in DME/F-12 medium supplemented with 100 μg/ml CHX after 1.5 h CHX preincubation. Electrophoretic mobility shift was monitored by immunoblotting. (B) Effect of in vivo deglycosylation of CFTR by PNGase F on the cell surface stability, as measured by anti–HA Ab binding assay with CHX treatment. (C) Effect of in vivo deglycosylation of CFTR by endo A on the cell surface stability of the core-glycosylated channel. HEK293S cells were treated with endo A (1/10, 0.2 mg/ml; or 1/5, 0.4 mg/ml) for 1 h after 3 h CHX chase, and CFTR was examined as in A and B. Error bars indicate SEM.

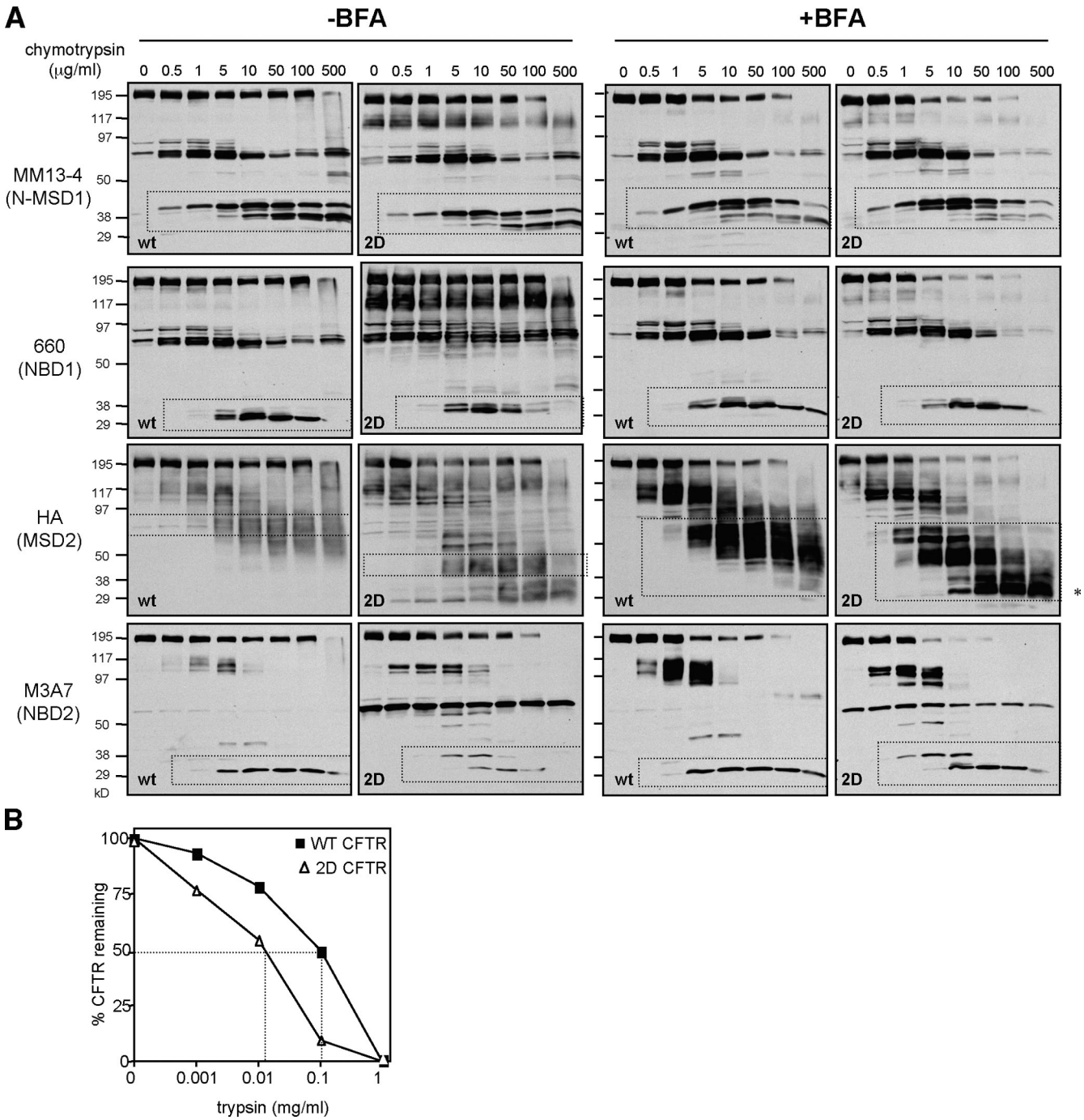

Figure S4. **Probing the mature wt and 2D-CFTR conformation by limited proteolysis in the ER and post-Golgi compartments.** (A) Limited chymotrypsin digestion of wt and 2D-CFTR was performed on isolated microsomes obtained from control and BFA-treated (10 μg/ml for 16 h) cells. Proteolytic digestion patterns were visualized by immunoblotting with domain-specific (shown in parentheses) anti-CFTR and anti–HA Ab. Dashed boxes designate the respective domain-containing fragments recognized by the domain-specific Ab. To eliminate the immature nonnative forms, cells were treated with CHX for 3 h before microsome isolation. (B) Densitometric analysis of the full-length wt and 2D-CFTR as a function of trypsin concentration using immunoblots shown in Fig. 8. The relative amount of CFTR was expressed as the percentage of the nondigested sample. The dotted lines indicate the trypsin concentration in which 50% of loss of the mature CFTR (full length) was achieved.

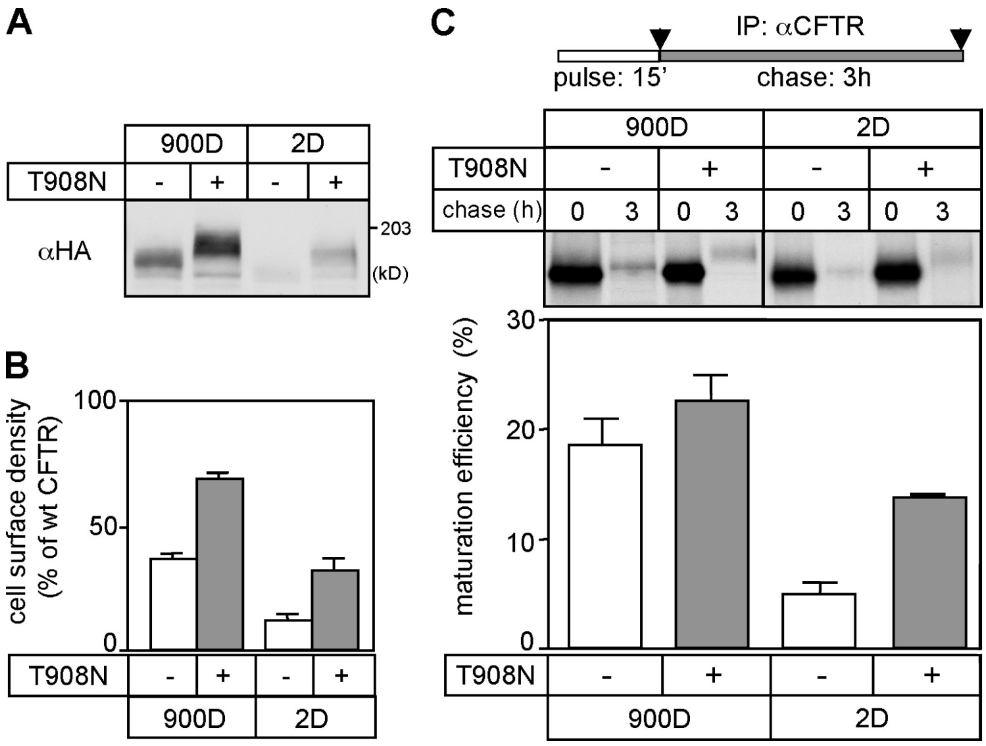

Figure S5. **The effect of transplanting an N-glycan chain on CFTR biogenesis.** (A and B) The effect of N-glycosylation site (T908N) on the CFTR expression and cell surface density were examined by immunoblotting (A) and anti–HA Ab binding assay (B; *n* = 5). (C) The effect of N-glycosylation site (T908N) insertion on the folding efficiency of the indicated CFTR variant was measured by the pulse-chase technique (*n* = 3–5). IP, immunoprecipitation. Error bars indicate SEM.